

AD-A174 009

A THEORY FOR THE SCALAR ROUGHNESS AND THE SCALAR
TRANSFER COEFFICIENTS OVER SNOW AND SEA ICE(U) COLD
REGIONS RESEARCH AND ENGINEERING LAB HANOVER NH

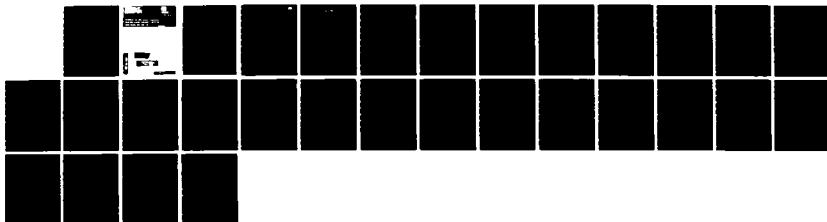
1/1

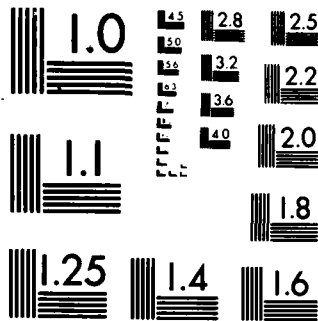
UNCLASSIFIED

E L ANDREAS SEP 86 CRREL-86-9

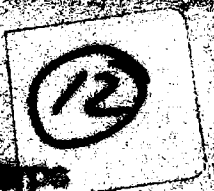
F/G 4/1

NL





MICROCOPY RESOLUTION TEST CHART
NATIONAL BUREAU OF STANDARDS-1963-A



60-100-1000
of 1000000

Cold Regions Research &
Engineering Laboratory

... roughness
... transfer coefficients
... ice

For conversion of SI metric units to U.S./British customary units of measurement consult ASTM Standard E380, Metric Practice Guide, published by the American Society for Testing and Materials, 1916 Race St., Philadelphia, Pa. 19103.

CRREL Report 86-9

September 1986



A theory for the scalar roughness and the scalar transfer coefficients over snow and sea ice

Edgar L. Andreas

Accession For	
NTIS	CRA&I
DTIC	TAB
Unannounced	<input type="checkbox"/>
Justification	<input type="checkbox"/>
By	
Distribution /	
Availability Codes	
Dist	Avail and/or Special
A-1	



Prepared for
OFFICE OF THE CHIEF OF ENGINEERS

Approved for public release; distribution is unlimited.

Unclassified

SECURITY CLASSIFICATION OF THIS PAGE (When Data Entered)

REPORT DOCUMENTATION PAGE		READ INSTRUCTIONS BEFORE COMPLETING FORM
1. REPORT NUMBER CRREL Report 86-9	2. GOVT ACCESSION NO. AD-A174089	3. RECIPIENT'S CATALOG NUMBER
4. TITLE (and Subtitle) A THEORY FOR THE SCALAR ROUGHNESS AND THE SCALAR TRANSFER COEFFICIENTS OVER SNOW AND SEA ICE		5. TYPE OF REPORT & PERIOD COVERED
7. AUTHOR(s) Edgar L Andreas		6. PERFORMING ORG. REPORT NUMBER
9. PERFORMING ORGANIZATION NAME AND ADDRESS U.S. Army Cold Regions Research and Engineering Laboratory Hanover, New Hampshire 03755-1290		10. PROGRAM ELEMENT, PROJECT, TASK AREA & WORK UNIT NUMBERS DA Project 4A161102AT24 Task FS, Work Unit 002
11. CONTROLLING OFFICE NAME AND ADDRESS Office of the Chief of Engineers Washington, D.C. 20314-1000		12. REPORT DATE September 1986
		13. NUMBER OF PAGES 26
14. MONITORING AGENCY NAME & ADDRESS (if different from Controlling Office)		15. SECURITY CLASS. (of this report) Unclassified
		15a. DECLASSIFICATION DOWNGRADING SCHEDULE
16. DISTRIBUTION STATEMENT (of this Report) Approved for public release; distribution is unlimited.		
17. DISTRIBUTION STATEMENT (of the abstract entered in Block 20, if different from Report)		
18. SUPPLEMENTARY NOTES		
19. KEY WORDS (Continue on reverse side if necessary and identify by block number) Heat and moisture exchange Surface processes Roughness lengths Turbulence Sea ice Snow		
20. ABSTRACT (Continue on reverse side if necessary and identify by block number) The bulk aerodynamic transfer coefficients for sensible (C_H) and latent (C_E) heat over snow and sea ice surfaces are necessary for accurately modeling the surface energy budget but are very difficult to measure. This report therefore presents a theory that predicts C_H and C_E as functions of the wind speed and a surface roughness parameter. The crux of the model is establishing the interfacial sublayer profiles of the scalars, temperature and water vapor, over aerodynamically smooth and rough surfaces. These interfacial sublayer profiles are derived from a surface-renewal model in which turbulent eddies continually sweep		

Unclassified

SECURITY CLASSIFICATION OF THIS PAGE (When Data Entered)

20. Abstract (cont'd).

down to the surface, transfer scalar contaminants across the interface by molecular diffusion, and then burst away. Matching the interfacial sublayer profiles with the usual semi-logarithmic inertial sublayer profiles yields the roughness lengths for temperature and water vapor. With these and a model for the drag coefficient over snow and sea ice based on actual measurements, the transfer coefficients are predicted. C_E is always a few percent larger than C_H . Both decrease monotonically with increasing wind speed for speeds above 1 m/s, and both increase at all wind speeds as the surface gets rougher. Both, nevertheless, are almost always between 1.0×10^{-3} and 1.5×10^{-3} .

→ 0.0010 and 0.0015.

7)

PREFACE

This report was prepared by Dr. Edgar L. Andreas, Physicist, of the Snow and Ice Branch, Research Division, U.S. Army Cold Regions Research and Engineering Laboratory. The work was supported by the Office of the Chief of Engineers, DA Project 4A161102AT24, *Research in Snow, Ice and Frozen Ground*; Task FS, *Fire Support*; Work Unit 002, *Winter Surface Boundary Layer Physics*.

The author thanks Brett Murphy for help with computing, William Bates for drafting the figures, Mark Hardenberg for editorial assistance, and Dr. V.J. Lunardini and Dr. Y.-C. Yen for reviewing the manuscript.

The contents of this report are not to be used for advertising or promotional purposes. Citation of brand names does not constitute an official endorsement or approval of the use of such commercial products.

CONTENTS

	Page
Abstract	i
Preface	iii
Nomenclature	v
Introduction	1
Aerodynamically rough surface	3
Aerodynamically smooth surface	8
Scalar transfer coefficients	13
Conclusions	16
Literature cited	17

ILLUSTRATIONS

Figure

1. Matching height over an aerodynamically rough surface as a function of roughness Reynolds number	6
2. Matching of interfacial and inertial sublayer profiles of temperature and water vapor over an aerodynamically rough surface	6
3. Model predictions for an aerodynamically rough surface compared with measured scalar roughness lengths for water vapor, thorium-B and camphor ...	7
4. Model predictions for an aerodynamically rough surface compared with the experimental data of Dipprey and Sabersky (1963)	8
5. Nondimensional matching height over an aerodynamically smooth surface as a function of σ	11
6. Matching of interfacial and inertial sublayer profiles of temperature and water vapor over an aerodynamically smooth surface	12
7. Current model predictions for an aerodynamically smooth surface compared with measured scalar roughness lengths for water vapor, thorium-B and heat, and with models by Brutsaert (1975b) and von Kármán (Goldstein 1965)	12
8. Model predictions of z_T/z_0 and z_Q/z_0 over snow and sea ice	13
9. Bulk transfer coefficients for sensible and latent heat over snow or sea ice as a function of the rms surface roughness (in centimetres) and the 10-m wind speed	15

TABLE

Table

1. Values of the coefficients in the polynomials that predict z_s/z_0 for temperature and water vapor	14
---------------------------------------------------------------------------------------------------------------	----

NOMENCLATURE

A	$\alpha_H k G \text{Pr}^{1/2} R_s^{1/2}$, a parameter in the equations modeling flow over a rough surface
a	10, a constant that relates eddy contact time to distance traveled
b_0, b_1, b_2	Coefficients of the polynomials that predict z_T/z_0 and z_Q/z_0 as functions of roughness Reynolds number
C_D	Drag coefficient at neutral stability
C_E	Bulk transfer coefficient for latent heat at neutral stability
C_H	Bulk transfer coefficient for sensible heat at neutral stability
c_p	Specific heat of air at constant pressure
D	Molecular diffusivity of heat
D_w	Molecular diffusivity of water vapor
G	5.6, a constant that relates the Kolmogorov time scale to t_r
h	Height at which inertial and interfacial sublayer profiles match
H_L	Latent heat flux
H_s	Sensible heat flux
K	A function of η_s , defined by eq 49
k	0.4, von Kármán's constant
K_e	Turbulent diffusivity of water vapor at neutral stability
K_H	Turbulent diffusivity of heat at neutral stability
K_M	Turbulent diffusivity of momentum at neutral stability
L_s	Latent heat of sublimation of ice
Pr	ν/D , Prandtl number
Q	Water vapor density
Q_r	Water vapor density at an arbitrary reference height r
Q_0	Water vapor density at the surface
q_*	$-H_L/L_s u_*$
r	Reference height
R_s	$u_* z_0/\nu$, roughness Reynolds number
S	Average profile value of an arbitrary scalar
S_0	Value of the arbitrary scalar at the surface
s_*	Equivalent to t_* or q_* for the arbitrary scalar
Sc	ν/D_w , Schmidt number
T	Potential temperature
t	Time
\bar{t}	Average eddy contact time over a smooth surface
T_b	Bulk temperature just above the interfacial sublayer
T_r	Potential temperature at an arbitrary reference level r
t_r	$G^2(z_0 \nu/u_*)^{1/2}$, fundamental eddy time scale over a rough surface
t_s	$85 \nu/u_*^2$, fundamental eddy time scale over a smooth surface
T_0	Surface temperature
t_*	$-H_s/\rho c_p u_*$

U	Longitudinal velocity
U_r	Velocity at an arbitrary reference height r
U_{10}	Velocity at a reference level of 10 m
u_*	$(\tau/\rho)^{1/2}$, friction velocity
x	Downwind distance
x_0	Distance over which an eddy remains in contact with a smooth surface
z	Height
z_Q	Roughness length for water vapor
z_s	Roughness length for an arbitrary scalar
z_T	Roughness length for temperature
z_0	Roughness length for velocity
α_E	K_E/K_M , inverse of the turbulent Schmidt number
α_H	K_H/K_M , inverse of the turbulent Prandtl number
β	Multiplicative constant in Charnock's (1955) equation
δ_T	$(D t_r)^{1/2}$, a fundamental length scale for flow over a rough surface
ϵ	Dissipation rate of turbulent kinetic energy
ζ	z/δ_T , nondimensional height over a rough surface
$\tilde{\zeta}$	h/δ_T , nondimensional matching height over a rough surface
η	$u_*^2 z^3/9 \nu D x$, nondimensional variable characterizing flow over a smooth surface
η_s	$u_* z^3/9 a \nu D t_s$, nondimensional height over a smooth surface
η_s	$u_* h^3/9 a \nu D t_s$, nondimensional matching height over a smooth surface
η_0	$u_* z^3/9 \nu D x_0$, another form of the nondimensional height over a smooth surface
ν	Kinematic viscosity of air
ξ	Root-mean-square surface elevation in centimetres
ρ	Density of air
σ	Ratio of kinematic viscosity to molecular diffusivity; equivalent to Pr for heat and Sc for water vapor
τ	Surface stress
ϕ_r	Distribution function for eddy contact time over a rough surface
ϕ_s	Distribution function for eddy contact time over a smooth surface

A Theory for the Scalar Roughness and the Scalar Transfer Coefficients Over Snow and Sea Ice

EDGAR L ANDREAS

INTRODUCTION

In the atmospheric surface layer at neutral stability, the velocity (U), potential temperature (T), and water vapor density (Q) profiles have the familiar, semi-logarithmic form,

$$\frac{U(z)}{u_*} = k^{-1} \ln(z/z_0), \quad (1)$$

$$\frac{T(z)-T_0}{t_*} = (\alpha_H k)^{-1} \ln(z/z_T), \quad (2)$$

$$\frac{Q(z)-Q_0}{q_*} = (\alpha_E k)^{-1} \ln(z/z_Q). \quad (3)$$

Here z is the height above the surface; k is von Kármán's constant (0.4); T_0 is the surface temperature; Q_0 is the water vapor density of air in saturation with a snow or sea ice surface at T_0 ; and $\alpha_H (= K_H/K_M)$ and $\alpha_E (= K_E/K_M)$ are the ratios of the scalar turbulent diffusivities, K_H and K_E , to the turbulent diffusivity for momentum K_M (e.g., Dyer 1974). The u_* , t_* , and q_* relate the profiles to the turbulent surface fluxes of momentum (τ) and sensible (H_s) and latent (H_L) heat:

$$\tau = \rho u_*^2, \quad (4)$$

$$H_s = -\rho c_p u_* t_*, \quad (5)$$

$$H_L = -L_s u_* q_*, \quad (6)$$

where ρ = air density

c_p = specific heat of air at constant pressure

L_s = latent heat of sublimation of ice.

Equations 1-3 define the roughness lengths. z_0 is the familiar roughness length for wind speed; z_T and z_Q are the roughness lengths for temperature and water vapor—the so-called scalar roughness lengths. z_0 is the height at which the semi-logarithmic velocity profile extrapolates to $U = 0$. Similarly, z_T and z_Q are the heights at which the semi-logarithmic temperature and water vapor profiles extrapolate to the surface values, T_0 and Q_0 , respectively. All are fictitious levels since the semi-logarithmic profiles are not valid clear down to the roughness lengths.

Knowing the roughness lengths is equivalent to knowing the bulk-aerodynamic transfer coefficients for momentum (C_D , the drag coefficient) and for the scalars, sensible (C_H) and latent (C_E) heat. After specifying a reference height r (henceforth taken as 10 m) to be the level where average values of wind speed (U_r), temperature (T_r), and humidity (Q_r) are measured, we define these transfer coefficients as

$$\tau = \rho C_D U_r^2, \quad (7)$$

$$H_s = \rho c_p C_H U_r (T_0 - T_r), \quad (8)$$

$$H_L = L_s C_E U_r (Q_0 - Q_r). \quad (9)$$

For neutral stability eq 1-6, in turn, relate these coefficients to the roughness lengths:

$$C_D = \frac{k^2}{[\ln(r/z_0)]^2}, \quad (10)$$

$$C_H = \frac{\alpha_H k C_D^{1/2}}{k C_D^{1/2} - \ln(z_T/z_0)}, \quad (11)$$

$$C_E = \frac{\alpha_E k C_D^{1/2}}{k C_D^{1/2} - \ln(z_Q/z_0)}. \quad (12)$$

Since correcting the transfer coefficients for stability effects is straightforward (e.g., Dardorff 1968, Large and Pond 1982), from here on all of my references to transfer coefficients will be to these neutral-stability ones. Clearly, from eq 10-12, $C_H = C_D$ only when $z_T = z_0$ and $\alpha_H = 1$; and $C_E = C_D$ only when $z_Q = z_0$ and $\alpha_E = 1$. I will show shortly that, contrary to the common assumption (e.g., Paulson 1970, Businger et al. 1971, Lettau 1979), z_T and z_Q rarely equal z_0 .

A typical goal of micrometeorology is to find C_D , C_H and C_E or, equivalently, z_0 , z_T and z_Q . These are fairly well known over the ocean but are still only poorly known over most other horizontally homogeneous surfaces. In particular, only C_D is well known over sea ice. The extensive set of C_D values that Banke et al. (1980) reported show that over sea ice C_D is an increasing function of the surface roughness. The roughness parameter here is the root-mean-square (rms) surface elevation along a line parallel to the wind direction and should not be confused with the roughness length z_0 . Leavitt et al. (1977) also found that C_D increased as the sea ice surface got rougher. Arya (1973, 1975) had theoretically predicted this increase in C_D with roughness, showing it to be a consequence of the form drag.

I know, however, of only two published attempts to measure C_H and C_E over snow or sea ice, those by Hicks and Martin (1972) over snow-covered Lake Mendota and by Thorpe et al. (1973) in the Beaufort Sea and in Robeson Channel. And the results are inconclusive. Hicks and Martin (1972) found $C_H = 0.9 \times 10^{-3}$ and $C_E = 2.5 \times 10^{-3}$, while Thorpe et al. (1973) reported $C_H = 1.2 \times 10^{-3}$ and $C_E = 0.55 \times 10^{-3}$. That is, in one case $C_H/C_E = 0.4$, and in the other $C_H/C_E = 2.2$. With only these few, contradictory values and without an adequate theory from which to estimate C_H and C_E in the absence of experimental values, sea ice modelers have had to rely on intuition or convention. Most (e.g., Parkinson and Washington 1979, Hibler 1980) have followed Maykut (1978) and assumed that C_H and C_E are constant—both equal to 1.75×10^{-3} . But eq 11 and 12 imply that C_H and C_E are not constant; they depend on the characteristics of the surface and on the wind speed, since C_D depends on the surface characteristics. Andreas and Ackley (1982) evidently were the first to point this out.

In this paper I will present a theoretical model for predicting C_H and C_E over snow and sea ice that relies on the empirical dependence of C_D on surface roughness reported by Banke et al. (1980). From eq 11 and 12 it is clear that to predict C_H and C_E I must also find z_T/z_0 and z_Q/z_0 . To do this I derive the scalar profiles in the interfacial sublayer over both aerodynamically rough and aerodynamically smooth surfaces. Matching these to the semi-logarithmic or inertial sublayer (Tennekes and Lumley 1972, p. 147) profiles (eq 2 and 3), I then solve for the scalar roughness. I treat snow and sea ice with the same model because sea ice is generally snow covered; the two surfaces are therefore aerodynamically similar.

AERODYNAMICALLY ROUGH SURFACE

With the ratio of kinematic viscosity to molecular diffusivity (σ), the roughness Reynolds number $R_* = u_* z_0/\nu$ customarily parameterizes wall-bounded shear flows. Although two flows may have different velocity or length scales or different kinematic viscosities (ν), they are dynamically similar if their roughness Reynolds numbers and their σ values are the same. Three dynamic regimes are possible, each characterized by a different R_* range (e.g., Businger 1973). If $R_* \leq e^{-2} = 0.135$, the surface roughness elements are imbedded in the viscous sublayer and the surface is *aerodynamically smooth*. If $R_* \geq 2.5$, the roughness elements poke through the viscous sublayer and the surface is *aerodynamically rough*. For $0.135 < R_* < 2.5$, the surface is in *transition*.

Brutsaert (1975a) and Liu et al. (1979) based models of the turbulent transfer over aerodynamically rough surfaces on a surface-renewal model (Danckwerts 1970, p. 100). Small eddies continually sweep into the interfacial sublayer, remain in contact with the surface for a short time, transferring heat and moisture by molecular diffusion, and then finally burst upward ahead of intruding new eddies. Grass (1971) suggested that while the eddies are in contact with the surface, they may be stagnant—trapped by the roughness elements. Brutsaert (1975a) thus assumed that over a rough surface the interfacial transfer of scalar properties is strictly a diffusion process. That is, using temperature as an example,

$$\frac{\partial T}{\partial t} = D \frac{\partial^2 T}{\partial z^2}, \quad (13)$$

where t is time. In eq 13 and in all that follow, we could use water vapor or any other scalar that obeys the same conservation equation as temperature (Hill 1978); the only changes would be in the molecular diffusivity D and in the other thermodynamic constants, such as the α 's or c_p and L_v . The boundary conditions on eq 13 are

$$\begin{aligned} T &= T_b & \text{for } z > 0, & \quad t = 0, \\ T &= T_b & \text{for large } z, & \quad t > 0, \\ T &= T_0 & \text{for } z = 0, & \quad t > 0, \end{aligned} \quad (14)$$

where T_b is the "bulk" temperature above the interfacial sublayer. Many standard texts show how to solve eq 13 with the boundary conditions of eq 14 (e.g., Duff and Naylor 1966, p. 118); the solution is

$$T(z,t) = (T_0 - T_b) \operatorname{erfc} \left[\frac{z}{2(Dt)^{1/2}} \right] + T_b, \quad (15)$$

where erfc is one minus the error function, erf (Abramowitz and Stegun 1965, p. 297).

Equation 15 models the diffusion into a single eddy. Because eddies continually sweep over the surface, we must integrate in time to find the average interfacial sublayer temperature profile. Brutsaert (1975a) and Liu and Businger (1975) used Danckwerts' (1951) distribution function,

$$\phi_T(t) = t_T^{-1} \exp(-t/t_T), \quad t > 0, \quad (16)$$

to model the fraction of surface area that has had eddies in contact for a time t . Here t_T is a time scale yet to be specified. The time-averaged temperature profile is thus

$$T(z) = \int_0^{\infty} T(z,t) \phi_T(t) dt. \quad (17)$$

Abramowitz and Stegun (1965, p. 303) show how to integrate the error function in eq 15; the solution of eq 17 is thus

$$T(z) = T_0 - (T_0 - T_b) [1 - \exp(-z/\delta_T)], \quad (18)$$

where

$$\delta_T = (D t_T)^{1/2}. \quad (19)$$

Khundzhua and Andreyev (1974) verified eq 18 experimentally in the aqueous sublayer in the Black Sea and related the length scale δ_T to the sensible heat flux. For air this relation is

$$\delta_T = \rho c_p D (T_0 - T_b) / H_s. \quad (20)$$

Actually, eq 20 is a necessary consequence of eq 18. H_s is related to the temperature gradient evaluated at the surface by

$$H_s = -\rho c_p D \left. \frac{\partial T}{\partial z} \right|_{z=0}. \quad (21)$$

But from eq 18, $\partial T / \partial z|_{z=0}$ is simply $(T_b - T_0) / \delta_T$; eq 20 thus follows from eq 21.

Substituting eq 5 for H_s in eq 20, we can write

$$T_0 - T_b = -u_* t_* \delta_T / D. \quad (22)$$

Substituting this into eq 18 yields a form for the temperature profile in the interfacial sublayer that is compatible with the inertial sublayer profile,

$$\frac{T(z) - T_0}{t_*} = (u_* \delta_T / D) [1 - \exp(-\zeta)]. \quad (23)$$

Here $\zeta = z / \delta_T$.

Brutsaert (1975a) and Liu et al. (1979) assumed that the time scale t_T in δ_T , eq 19, is proportional to the Kolmogorov time scale $(\nu/\epsilon)^{1/2}$, where ϵ is the dissipation rate of turbulent kinetic energy. Formalizing this assumption by defining a proportionality constant G and setting $\epsilon = u_*^3 / z_0$ (Liu et al. 1979), we have

$$t_r = G^2(z_0 \nu / u_*^3)^{1/2}, \quad (24)$$

or

$$\delta_T / z_0 = G \text{Pr}^{-1/2} R_*^{-1/4}, \quad (25)$$

where $\text{Pr} = \nu / D$ is the Prandtl number. Liu et al. (1979) estimated $G = 9.3$ on the basis of data reported by Mangarella et al. (1973) for flow over wind waves. Since snow or sea ice surfaces are less compliant than water, this value of G may not be appropriate. In fact, in evaluating G , Liu et al. (1979) also considered data reported by Chamberlain (1968) that imply $G = 5.6$ for flows over various solid surfaces. My model, with this G value, fits data collected over various solid surfaces much better than with $G = 9.3$. Evidently, the proportionality constant in eq 24 and 25 depends on whether the surface is firm or compliant.

With eq 25 we can now simultaneously solve eq 2 and 23 to find z_T . This is where I diverge from Brutsaert (1975a). I will simply match both the temperature profiles and their first derivatives at $z = h$. The temperature and the heat flux will therefore both be continuous from the interfacial to the inertial sublayer. With these profile and first-derivative equations, I can find the two unknowns h and z_T . Brutsaert (1975a) never computed the interfacial sublayer profile; instead he solved for z_T by matching the interfacial and inertial sublayer fluxes at the arbitrary level $h = 7.39z_0$. Although they do not say explicitly, Liu et al. (1979) used the method of solution that I am proposing. They, however, set $G = 9.3$ and $\alpha_H = \alpha_E = 1.14$, while I use $G = 5.6$ and $\alpha_H = \alpha_E = 1.0$.

Matching the profiles eq 2 and 23 at $z = h$ gives

$$\ln \hat{\xi} - \ln(z_0 / \delta_T) - \ln(z_T / z_0) = A[1 - \exp(-\hat{\xi})], \quad (26)$$

where

$$\hat{\xi} = h / \delta_T, \quad (27)$$

and

$$A = \alpha_H k G \text{Pr}^{1/2} R_*^{1/4}. \quad (28)$$

Matching the first derivatives at $\hat{\xi}$ yields

$$\hat{\xi} \exp(-\hat{\xi}) = A^{-1}. \quad (29)$$

I do not need to worry here or in eq 26 about the stability of the atmospheric surface layer and its effects on the inertial sublayer profiles. We will see that the matching level is well below the region where atmospheric stability affects the semi-logarithmic profiles (Bradley 1972). Notice, eq 29 has a solution only for $A > 2.72$. Substituting it into eq 26 gives a formal expression for z_T / z_0 ,

$$z_T / z_0 = \hat{\xi} (\delta_T / z_0) \exp[\hat{\xi}^{-1} - A]. \quad (30)$$

Here A and δ_T are functions only of Pr and R_* . We solve for $\hat{\xi}$ by using Newton's method to find the zeroes in eq 29 as functions of Pr and R_* . Figure 1 shows $h / z_0 = (\hat{\xi} \delta_T / z_0)$ for both temperature and water vapor when $R_* = 10$. The values are much smaller than the constant that Brutsaert (1975a) used. He chose $h = 7.39z_0$ because this is approximately the

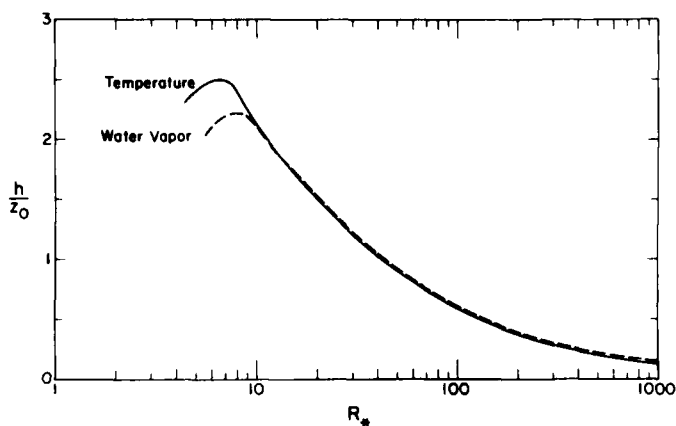


Figure 1. Matching height over an aerodynamically rough surface as a function of roughness Reynolds number. For temperature, $\sigma = 0.71$; for water vapor, $\sigma = 0.63$.

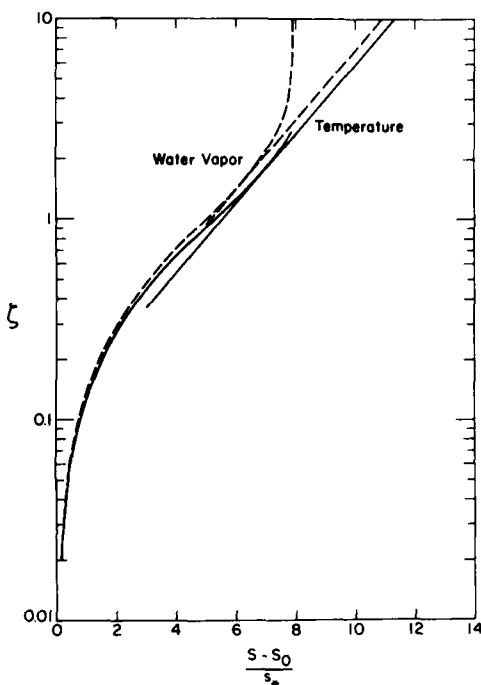


Figure 2. Matching of interfacial and inertial sublayer profiles of temperature ($\sigma = 0.71$) and water vapor ($\sigma = 0.63$) over an aerodynamically rough surface for $R_* = 10$.

height of the roughness elements. By implying that the roughness elements protrude above the interfacial sublayer, Figure 1 is, thus, consistent with our conceptual model of molecular diffusion into stagnant eddies.

Figure 2 shows the transition of temperature and water vapor profiles from the interfacial to the inertial sublayer. Both the profiles and their first derivatives are continuous. The vertical fluxes of sensible and latent heat are, therefore, also continuous.

Figure 3 compares predictions of my model for the scalar roughness, z_s , with experimental data from Owen and Thomson (1963) and Chamberlain (1966, 1968). All the data sets are from wind tunnel measurements and represent three different σ values. Chamberlain (1966) studied water vapor transfer over toweling and artificial grass ($\sigma = 0.62$ at $\sim 20^\circ\text{C}$). Because the grass, however, had a roughness length of 1.0 cm—much larger than that typical of snow or sea ice (Untersteiner and Badgley 1965, Banke et al. 1980, Schmidt 1982)—and roughness elements unlike those of snow or sea ice, I have not included those data. Chamberlain (1968) collected his thorium-B ($\sigma = 2.78$) and water vapor data over a host of two- and three-

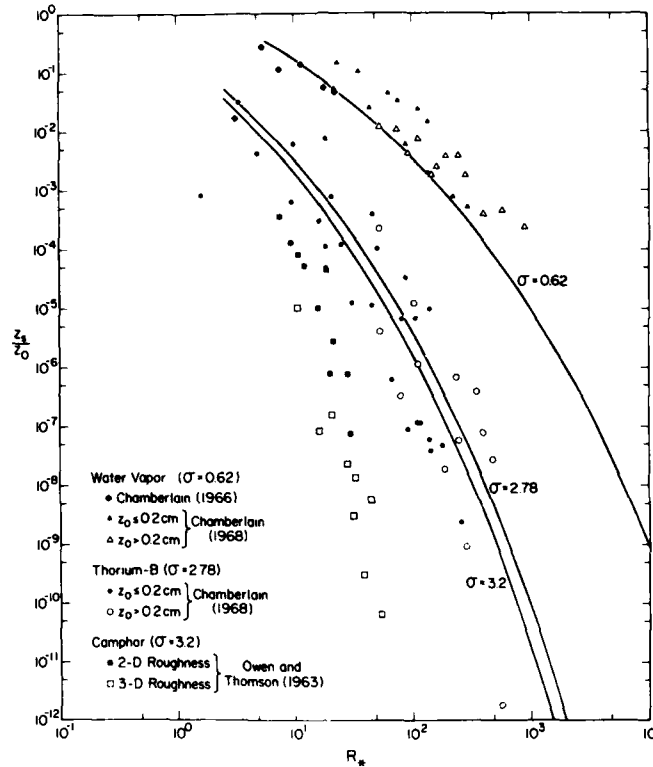


Figure 3. Model predictions for an aerodynamically rough surface compared with measured scalar roughness lengths for water vapor, thorium-B and camphor.

dimensional roughness elements, some with roughness lengths as large as 0.6 cm. In the figure I have indicated the data for surfaces with $z_0 > 0.2$ cm—roughly the maximum sea ice roughness that Banke et al. (1980) reported. No systematic difference between large and small roughness lengths is evident, however. Owen and Thomson (1963) looked at the transfer of camphor ($\sigma = 3.2$) over glass surfaces with two- and three-dimensional roughness.

Measuring z_s/z_0 is difficult under any circumstances—even in a wind tunnel—because, as eq 1 and 2 show with temperature for example, we have to know u_* , t_* and z_0 . Chamberlain (1968) explained that his z_0 values alone may have been in error by 50%. The scatter of the data in Figure 3 is, thus, not surprising. In view of this uncertainty, the model predictions are quite good. The model reproduces the R_* -dependence at constant σ very well and has z_s/z_0 decreasing with increasing σ , as the data do. Only the z_s/z_0 data from Owen and Thomson (1963) deviate significantly from model predictions. I can only speculate that significant measurement errors crept into their results. For example, Owen and Thomson (1963) determined the camphor flux by weighing a test section of the floor of their wind tunnel before and after each experimental run. The 7-cm-square glass test section must have been at least 100 g, but the typical difference in camphor coating before and after each of their runs was only 0.1 g. Their flux measurement, therefore, likely had low precision. Secondly, as camphor was subliming from the floor of the wind tunnel during a run, the z_0 value may have been changing.

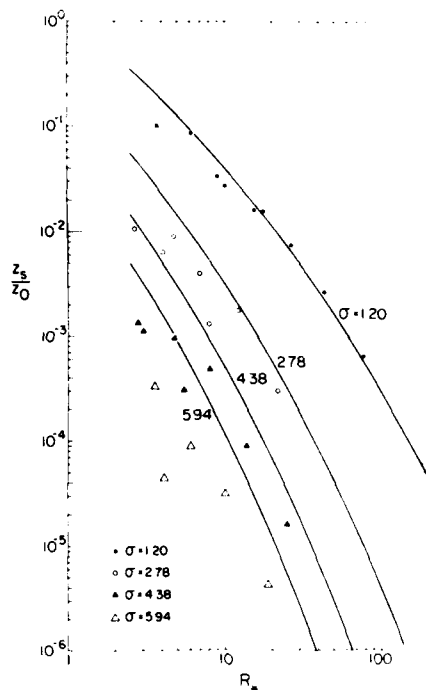


Figure 4. Model predictions for an aerodynamically rough surface compared with the experimental data of Dipprey and Sabersky (1963).

Figure 4 compares model predictions of z_s/z_0 with the data of Dipprey and Sabersky (1963), who investigated heat transfer in water-filled pipes. Pipe flow may not seem to be a good experimental model for flow in the atmospheric surface layer, but the two are, in fact, mathematically equivalent. Flow in pipes is characterized by a viscous sublayer near the wall and a semi-logarithmic inertial sublayer further from the wall (Schlichting 1968, p. 578; Tennekes and Lumley 1972, p. 149), just like my model for the atmospheric surface layer. Figure 4 confirms the validity of the comparison. Dipprey and Sabersky (1963) varied σ by changing the water temperature; the model fits their data extremely well for $\sigma = 1.20$ and reasonably well at the other σ values. For all of the σ values in the figure, the difference between the data and the model predictions tends to decrease as R_* increases. This suggests some experimental imprecision at low flow rates. Nevertheless, as in Figure 3, the model does reproduce the general trends in the data. In summary, my model seems to be an adequate fit to the available data that are most representative of an aerodynamically rough snow or sea ice surface.

AERODYNAMICALLY SMOOTH SURFACE

Brutsaert (1975a) also modeled scalar transfer over an aerodynamically smooth surface by again postulating a surface-renewal mechanism. Over a smooth surface, however, an impinging eddy remains in motion; the transfer is thus governed by an advective diffusion model,

$$U(z) \frac{\partial T}{\partial x} = D \frac{\partial^2 T}{\partial z^2}, \quad (31)$$

where $U(z)$ is the velocity profile in the viscous sublayer. The boundary conditions on eq 31 are

$$\begin{aligned} T &= T_b & \text{for } z > 0, & \quad x = 0, \\ T &= T_b & \text{for large } z, & \quad x > 0, \\ T &= T_0 & \text{for } z = 0, & \quad x > 0. \end{aligned} \quad (32)$$

In the viscous sublayer, $z u_* / \nu < 5$,

$$U(z) = u_*^2 z / \nu \quad (33)$$

(e.g., Monin and Yaglom 1971, p. 270; Brutsaert 1975a). On substituting eq 33 into eq 31 and making the change of variables

$$\eta = \frac{u_*^2}{9 \nu D} \frac{z^3}{x} \quad (34)$$

suggested by Kestin and Persen (1962), we get the equation

$$(\eta + \frac{1}{3}) \frac{\partial T}{\partial \eta} + \eta \frac{\partial^2 T}{\partial \eta^2} = 0. \quad (35)$$

The solution that satisfies the boundary conditions is (Kestin and Persen 1962)

$$T(\eta) = T_0 - (T_0 - T_b) \frac{\gamma(\frac{1}{3}, \eta)}{\Gamma(\frac{1}{3})}, \quad (36)$$

where Γ is the gamma function and γ is the incomplete gamma function (Abramowitz and Stegun 1965, p. 255 and 260, respectively). Although Brutsaert (1975a) posed eq 31 with the boundary conditions of eq 32, he solved only for $\partial T / \partial z$ at $z = 0$.

We next impose the assumptions of the surface-renewal model—that the eddy is in contact with the surface only for $0 \leq x \leq x_0$. Averaging $T(\eta)$ over this distance yields

$$T(z, x_0) = T_0 - \frac{(T_0 - T_b)}{\Gamma(\frac{1}{3})} [\gamma(\frac{1}{3}, \eta_0) + \eta_0 \Gamma(-\frac{2}{3}, \eta_0)], \quad (37)$$

where

$$\Gamma(-\frac{2}{3}, \eta_0) = \Gamma(-\frac{2}{3}) - \gamma(-\frac{2}{3}, \eta_0) \quad (38)$$

is another form of the incomplete gamma function, and

$$\eta_0 = \frac{u_*^2}{9 \nu D} \frac{z^3}{x_0}. \quad (39)$$

To remove the explicit dependence on x_0 in eq 37, we have to average over all possible values of x_0 . Brutsaert (1975a) suggested setting

$$x_0 = a u_* l, \quad (40)$$

where a is a constant, and then using eq 16 for the distribution function of t . In other words, we would again have the integral eq 17, with eq 37 substituted for eq 15. If Brutsaert had attempted this integration, he would have found the integral infinite. The reason is that the distribution function (eq 16) is not the appropriate one over a smooth surface. The work of Kim et al. (1971) suggested that for smooth surfaces the eddy-contact time has the distribution

$$\phi_s(t) = (t/t_s^2) \exp(-t/t_s), \quad t > 0, \quad (41)$$

where t_s is a new time scale. The average contact time is thus $\bar{t} = 2t_s$. In addition, from Figures 23 and 24 in Kim et al. (1971) I derived

$$\bar{t} = 170 \nu/u_*^2, \quad (42)$$

or

$$t_s = 85 \nu/u_*^2. \quad (43)$$

Notice, since ν/u_* is the appropriate scaling length in the viscous sublayer over a smooth surface (Tennekes and Lumley 1972, p. 152), ν/u_*^2 is the only reasonable time scale there.

Substituting eq 37 and 41 into the time-averaging integral, eq 17, rearranging arguments a little, and defining

$$\eta_s = \frac{u_* z^3}{9a\nu Dt_s}, \quad (44)$$

we derive an expression for the average profile in the interfacial sublayer,

$$T(z) = T_0 - \frac{(T_0 - T_b)\eta_s^2}{\Gamma(1/3)} \int_0^\infty [\eta_0^{-1}\gamma(1/3, \eta_0) + \Gamma(-2/3, \eta_0)] \eta_0^{-2} \exp(-\eta_s/\eta_0) d\eta_0. \quad (45)$$

The method of steepest descent (e.g., Dennery and Krzywicki 1967) is useful for approximating such difficult integrals; it yields

$$T(z) = T_0 - \frac{(T_0 - T_b)}{\Gamma(1/3)} \{0.960\gamma(1/3, \eta_s/2) + 1.383\eta_s[\gamma(1/3, \eta_s) - \Gamma(1/3) + \eta_s^{-1/3} \exp(-\eta_s)]\}. \quad (46)$$

This, to my knowledge, is the first derivation of the interfacial sublayer profile of a scalar over an aerodynamically smooth surface that is based on surface-renewal concepts.

As with the rough-surface case, we have to eliminate T_b in eq 46 to match the interfacial and inertial sublayer profiles. Again, we know how the surface flux is related to the profile—simply by eq 21. Using this and substituting eq 43 for t_s in eq 46 we find

$$T_0 - T_b = 1.519(85a)^{1/3} \text{Pr}^{1/3} t_*, \quad (47)$$

Hence,

$$T(z) = T_0 + 1.458(85a)^{1/3} \text{Pr}^{1/3} t_* K(\eta_s), \quad (48)$$

where

$$K(\eta_s) = \Gamma(1/3)^{-1} [\gamma(1/3, \eta_s/2) + 1.44[\gamma(1/3, \eta_s) - \Gamma(1/3) + \eta_s^{-1/3} \exp(-\eta_s)]] \quad (49)$$

Notice, with η_s , eq 43, substituted into η_s , eq 44, and recognizing that over a smooth surface

$$z_0 = e^{-2} \nu/u_* \quad (50)$$

(Tennekes and Lumley 1972, p. 157), η_s becomes

$$\eta_s = \frac{e^{-6}}{9 \cdot 85 \cdot a} \text{Pr} \left(\frac{z}{z_0} \right)^3 \quad (51)$$

Matching the profiles at $z = h$ or at

$$\hat{\eta}_s = \frac{e^{-6}}{9 \cdot 85 \cdot a} \text{Pr} \left(\frac{h}{z_0} \right)^3 \quad (52)$$

we get

$$\frac{1}{3} \ln \hat{\eta}_s + \frac{1}{3} \ln \left(\frac{9 \cdot 85 \cdot a}{e^{-6} \text{Pr}} \right) - \ln(z_T/z_0) = 1.458 \alpha_H k(85a)^{1/3} \text{Pr}^{1/3} K(\hat{\eta}_s) \quad (53)$$

And matching the slopes there, too,

$$\begin{aligned} \frac{1}{3} = & 1.458 \alpha_H k(85a)^{1/3} \text{Pr}^{1/3} \Gamma(1/3)^{-1} [(\hat{\eta}_s/2)^{1/3} \exp(-\hat{\eta}_s/2) \\ & + 1.44 \hat{\eta}_s [\gamma(1/3, \hat{\eta}_s) - \Gamma(1/3) + \frac{1}{3} \hat{\eta}_s^{-1/3} \exp(-\hat{\eta}_s)]] \end{aligned} \quad (54)$$

I again solve eq 54 for $\hat{\eta}_s$ by Newton's method and then find z_T/z_0 from eq 53,

$$z_T/z_0 = \hat{\eta}_s^{1/3} \left(\frac{9 \cdot 85 \cdot a}{e^{-6} \text{Pr}} \right)^{1/3} \exp[-1.458 \alpha_H k(85a)^{1/3} \text{Pr}^{1/3} K(\hat{\eta}_s)] \quad (55)$$

The constant a is yet to be specified. The viscous sublayer velocity profile, eq 33, is approximately valid from the surface to the lower boundary of the inertial sublayer at $30 \nu/u_*$ (Tennekes and Lumley 1972, p. 160). Therefore, integrating this profile from zero to $30 \nu/u_*$ should yield an average velocity \bar{U} for the viscous sublayer. That average is $\bar{U} = 15u_*$. Comparing this result with eq 40, we see that a should be roughly 15. I have found that the value $a = 10$ fits the available data best.

Figure 5 shows model calculations of the nondimensional matching height as a function of

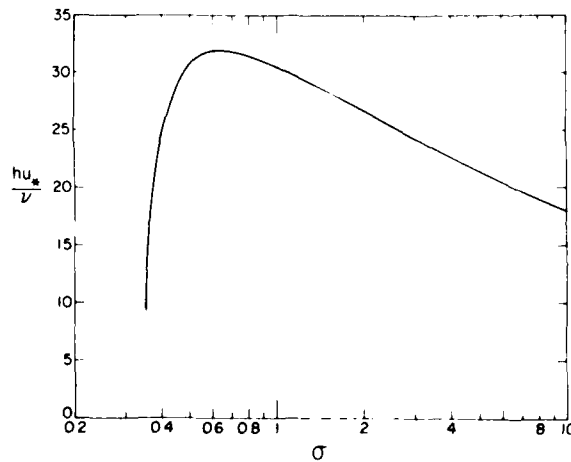


Figure 5. Nondimensional matching height over an aerodynamically smooth surface as a function of σ .

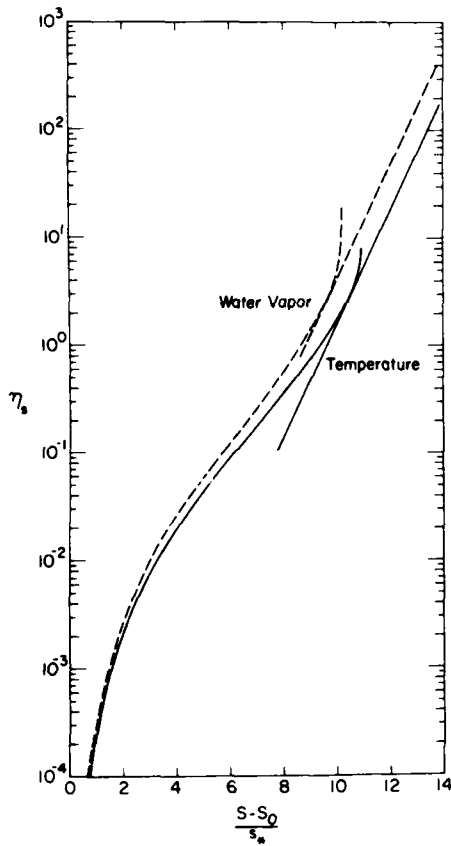


Figure 6. Matching of interfacial and inertial sublayer profiles of temperature ($\sigma = 0.71$) and water vapor ($\sigma = 0.63$) over an aerodynamically smooth surface.

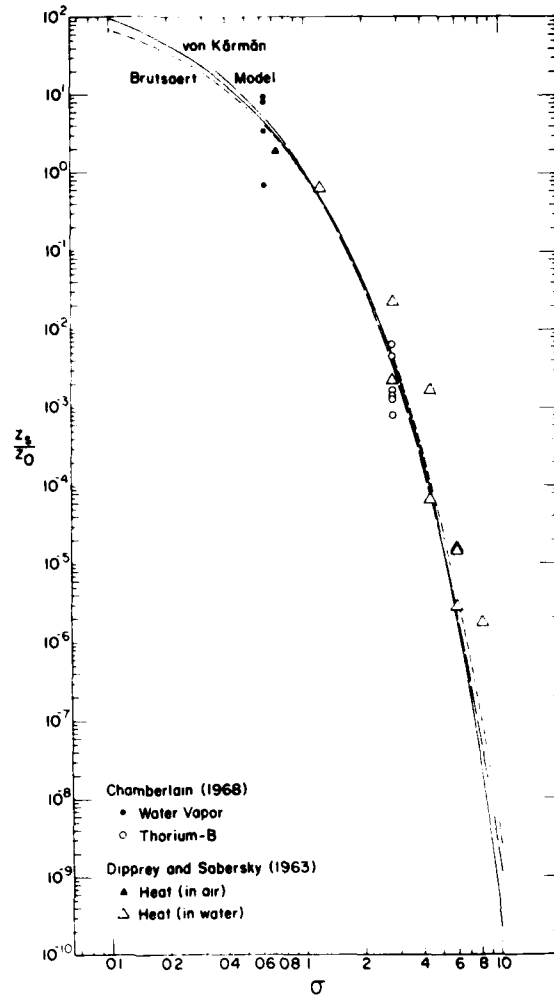


Figure 7. Current model predictions for an aerodynamically smooth surface compared with measured scalar roughness lengths for water vapor, thorium-B and heat, and with models by Brutsaert (1975b) and von Kármán (Goldstein 1965).

σ . For temperature and water vapor, the value $h u_* / \nu$ is about 32. Brutsaert (1975a) did his matching by assuming that $h u_* / \nu = 30$ for all values of σ . Figure 6 shows the matching of interfacial and inertial sublayer profiles for temperature and water vapor over an aerodynamically smooth surface. As with the aerodynamically rough surface, both profiles and their first derivatives are continuous at h .

Finally, Figure 7 compares my model predictions with the scanty data available from flows over smooth surfaces. In the figure the data from Chamberlain (1968) are the "smooth surface" values from his Tables 2 and 3. The data from Dipprey and Sabersky (1963) are from their smooth pipe (E-3, their Fig. 5) and from their three rough pipes (their Fig. 6-8) for runs when $R_* \leq 0.135$. The fourth-order polynomial

$$\ln(z_s/z_0) = 0.0399 - 3.92 \ln \sigma - 1.22(\ln \sigma)^2 - 0.254(\ln \sigma)^3 - 0.0748(\ln \sigma)^4 \quad (56)$$

is a good representation of my model results for $0.35 \leq \sigma \leq 10.0$. The figure also shows Brutsaert's (1975b) prediction,

$$z_s/z_0 = \exp[-k(13.6\sigma^{3/4} - 13.5)], \quad (57)$$

and von Kármán's (Goldstein 1965, p. 657; Monin and Yaglom 1971, p. 342),

$$z_s/z_0 = \exp[-5k\{(\sigma-1) + \ln[1 + 0.83(\sigma-1)]\}]. \quad (58)$$

The three models are so close that, with the scatter in the experimental data and their sparsity, it is impossible to decide which is best.

Notice in Figure 7 that all three models predict $z_s/z_0 \cong 1$ for $\sigma = 1$. This is compatible with the Reynolds analogy—that over an aerodynamically smooth surface, where the roughness elements cannot cause momentum transfer through pressure forces, the transfer must be identical for momentum and for a scalar contaminant with $\sigma = 1$. von Kármán (Goldstein 1965, p. 657) explicitly assumed the validity of the Reynolds analogy and thus forced his model to predict $z_s/z_0 = 1$ at $\sigma = 1$. While neither Brutsaert (1975a, b) nor I made this assumption, his model predicts $z_s/z_0 = 0.96$ at $\sigma = 1$, and mine predicts $z_s/z_0 = 1.04$.

SCALAR TRANSFER COEFFICIENTS

With the results of the last two sections we can specify z_T/z_0 and z_Q/z_0 over snow or sea ice for all R_* (Fig. 8). Since temperatures will be 0°C or less, I take the Prandtl number (ν/D) as 0.71 and the Schmidt number (ν/D_w) as 0.63, with values for the molecular diffusivity of water vapor, D_w , taken from Pruppacher and Klett (1978, p. 413). In R_* I evaluate ν at -5°C . Because the model predicts z_s/z_0 only over aerodynamically smooth and rough surfaces, to obtain z_s/z_0 values in the transition region, I did a log-log interpolation between model results at $R_* = 0.135$ and $R_* = 2.5$.

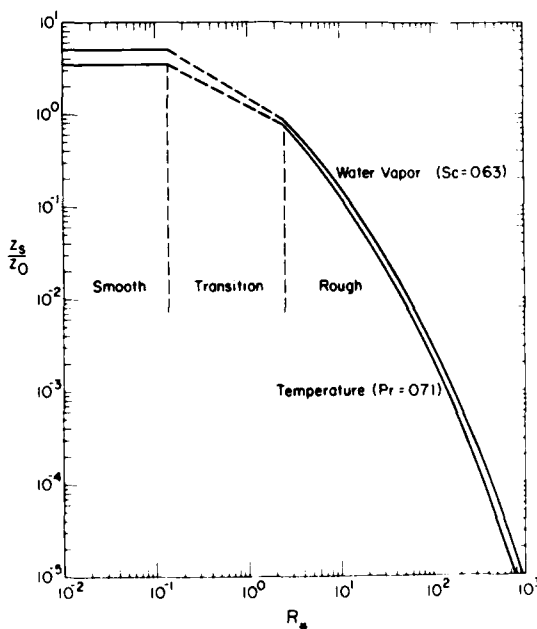


Figure 8. Model predictions of z_T/z_0 and z_Q/z_0 over snow and sea ice.

Table 1. Values of the coefficients in the polynomials (eq 59) that predict z_s/z_0 for temperature ($\sigma = 0.71$) and water vapor ($\sigma = 0.63$).

	$R_* \leq 0.135$	$0.135 < R_* < 2.5$	$2.5 \leq R_* \leq 1000$
Temperature			
b_0	1.250	0.149	0.317
b_1	—	-0.550	-0.565
b_2	—	—	-0.183
Water vapor			
b_0	1.610	0.351	0.396
b_1	—	-0.628	-0.512
b_2	—	—	-0.180

Figure 8 shows that z_Q is slightly larger than z_T at all roughness Reynolds numbers. As Figures 3, 4 and 7 imply, this is strictly an effect of the difference in molecular diffusivities. Both z_T and z_Q are usually less than z_0 ; z_T/z_0 and z_Q/z_0 become less than one in the transition region and decrease monotonically in the aerodynamically rough region. Thus, z_T and z_Q are virtually always less than z_0 in natural flows.

Several recent models predicted scalar transfer over aerodynamically rough surfaces. The model by Garratt and Hicks (1973)—which is just the empirical equation that Owen and Thomson (1963) derived—predicts z_s/z_0 values generally five times larger than my model. The predictions of z_s/z_0 by Liu et al. (1979), which admittedly are for a water surface, are almost an order of magnitude smaller than mine. Brutsaert's (1975b) model predicts z_s/z_0 values smaller than mine for $R_* < 20$ but values fairly close to mine for larger R_* .

For facilitating computer modeling, I have fitted the model results in Figure 8 with polynomials of the form

$$\ln(z_s/z_0) = b_0 + b_1 \ln R_* + b_2 (\ln R_*)^2. \quad (59)$$

Table 1 lists the coefficients for smooth, transition and rough surfaces.

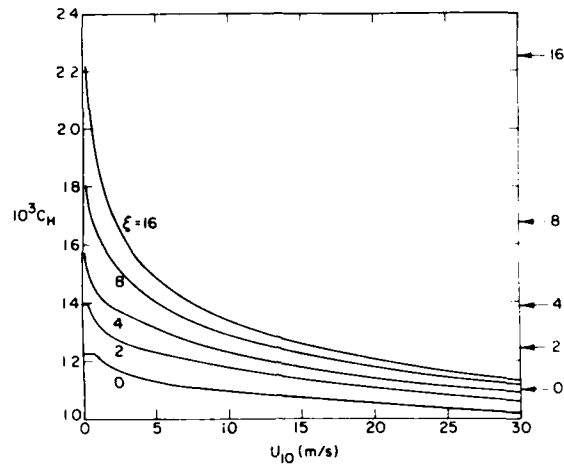
As eq 11 and 12 show, if we know z_T/z_0 , z_Q/z_0 and C_D , we can find C_H and C_E . The model for C_D presented by Banke et al. (1980) synthesizes a representative collection of C_D values measured over a host of sea ice surfaces. Their empirical result,

$$10^3 C_D = 1.10 + 0.072 \xi, \quad (60)$$

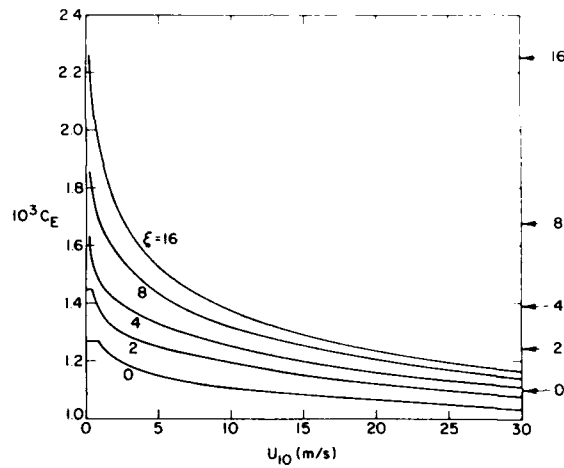
parameterizes the drag coefficient in terms of the rms surface roughness ξ in centimetres. Banke et al. (1980) found ξ by measuring the surface elevation at 1-m intervals for several hundred metres upwind of their instruments. Integrating the power spectrum of these data over wavelengths less than 13 m yielded ξ^2 . The z_0 values reported by Schmidt (1982) for blowing snow and those summarized by Chamberlain (1983) for drifting snow and sand are generally in the range reported by Banke et al. (1980); hence, we assume that eq 60 is a valid model for snowfields, too.

Kind (1976) and Chamberlain (1983) suggested that roughness lengths for snow and sand obey Charnock's (1955) relation,

$$z_0 = \beta u_*^2/g, \quad (61)$$



a. C_H .



b. C_E .

Figure 9. Bulk transfer coefficients for sensible (C_H) and latent (C_E) heat over snow or sea ice as a function of the rms surface roughness (in centimetres) and the 10-m wind speed U_{10} . The arrows on the right show C_D for the indicated ξ value.

where g is the acceleration of gravity and β is a dimensionless constant in the range 0.010–0.016. Through eq 10, eq 61 would yield C_D ; but because eq 60 parameterizes the form drag, which as I explained is an important effect over sea ice, I prefer eq 60 to 61.

The routine for estimating C_H and C_E is first to select a ξ value; this value then defines C_D from eq 60. C_D , in turn, has a one-to-one relationship with z_0 through eq 10. Finally, we compute R_* from

$$R_* = U_{10} C_D^{1/2} z_0 / \nu, \quad (62)$$

where U_{10} is the wind speed at 10 m. Substituting R_* into eq 59, we use the resulting z_T/z_0 and z_Q/z_0 values to compute C_H and C_E for a 10-m reference height from eq 11 and 12. Figure 9 shows C_H and C_E as functions of ξ and U_{10} . Remember again, C_D , C_H and C_E are the values at neutral stability.

According to Figure 9, C_E is always 1–3% larger than C_H . And except for very low wind speed, when the surface is aerodynamically smooth or in transition, both are smaller than C_D .

The form of the C_H and C_E functions in Figure 9 is different from that predicted by Kondo (1975) and by Liu et al. (1979) for C_H and C_E over the ocean. According to Figure 9, C_H and C_E are monotonically decreasing functions of wind speed, except at very low speeds over smooth surfaces where they are constant. Kondo (1975) predicted that over the ocean C_H and C_E have minimums at about 2 m/s and then increase gradually as the wind speed increases. Liu et al. (1979) predicted that C_H and C_E have local minimums at roughly 2 m/s, local maximums at about 5 m/s, then decrease slowly for increasing wind speeds. The basic reason for the differences between my model and these is that over the ocean C_D has a wind speed dependence. No such wind speed dependence has been established for the drag coefficient over snow or sea ice.

In Figure 9, C_H and C_E are generally between 1.0×10^{-3} and 1.5×10^{-3} . Only over the roughest surfaces—and then only at low wind speeds—are C_H and C_E larger than 1.5×10^{-3} . C_H and C_E go below 1.0×10^{-3} only at unusually high wind speeds. The model predictions therefore cast doubt on the scalar transfer coefficients reported by Hicks and Martin (1972) and Thorpe et al. (1973). For wind speeds of about 3 m/s, Hicks and Martin (1972) found average values of C_H and C_E over snow-covered Lake Mendota to be 0.9×10^{-3} and 2.5×10^{-3} respectively. Over ice in the Beaufort Sea, Thorpe et al. (1973) found averages of $C_H = 1.2 \times 10^{-3}$ and $C_E = 0.55 \times 10^{-3}$ for winds ranging from 5 to 10 m/s. Only the C_H measurement by Thorpe et al. (1973) is compatible with theoretical predictions.

I do not mean here to deprecate the efforts of these scientists; measuring C_H and C_E over natural snow and sea ice surfaces is an important but extremely difficult job. First, you have to measure u_* either by measuring the vertical velocity profile or by measuring τ directly. Next, you must measure t_* and q_* —again, either by measuring the vertical profiles of temperature and water vapor or by measuring H_s and H_L directly. These are necessary not only for finding C_H and C_E but also for making stability corrections. Last, and probably most important, is the measurement of T_0 and Q_0 . Since $T_0 - T_r$ and $Q_0 - Q_r$ are rarely large over frozen surfaces, the T_0 and Q_0 measurements must be precise. But because the surface is ill-defined, simply deciding what level over the snow corresponds to T_0 and Q_0 is a problem; finding instruments capable of measuring T_0 and Q_0 without disturbing the integrity of the surface is another. Consequently, the most careful flux measurements are of little value for specifying C_H and C_E if T_0 and Q_0 are not measured as carefully.

CONCLUSIONS

I have modeled the transfer of the passive scalar contaminants temperature and water vapor over aerodynamically rough and smooth snow and sea ice surfaces. The basis of the model is a smooth matching of interfacial and inertial sublayer profiles. The inertial sublayer profile has the usual semi-logarithmic form; I derive the interfacial sublayer profiles over smooth and rough surfaces on the basis of a turbulent surface-renewal model. This, I think, is the first such derivation of the interfacial sublayer profile for a passive scalar over an aerodynamically smooth surface.

The model yields values of z_T/z_0 and z_Q/z_0 as functions of the roughness Reynolds number. Using these values and the empirical model for the drag coefficient over sea ice given by Banke et al. (1980), I predict the bulk coefficients for sensible (C_H) and latent (C_E) heat at neutral stability over snow and sea ice. These depend on the wind speed and on a surface roughness parameter. C_E is 1–3% larger than C_H ; at wind speeds greater than 3 m/s both are virtually always between 1.0×10^{-3} and 1.5×10^{-3} . Only at low wind speeds—which usually do not persist—and over very rough surfaces are C_H and C_E larger than 1.5×10^{-3} .

LITERATURE CITED

- Abramowitz, M. and I.A. Stegun** (Ed.) (1965) *Handbook of Mathematical Functions*. New York: Dover.
- Andreas, E.L. and S.F. Ackley** (1982) On the differences in ablation seasons of Arctic and Antarctic sea ice. *Journal of the Atmospheric Sciences*, **39**: 440-447.
- Arya, S.P.S.** (1973) Contribution of form drag on pressure ridges to the air stress on Arctic ice. *Journal of Geophysical Research*, **78**: 7092-7099.
- Arya, S.P.S.** (1975) A drag partition theory for determining the large-scale roughness parameter and wind stress on the Arctic pack ice. *Journal of Geophysical Research*, **80**: 3447-3454.
- Banke, E.G., S.D. Smith and R.J. Anderson** (1980) Drag coefficients at AIDJEX from sonic anemometer measurements. In *Sea Ice Processes and Models* (R.S. Pritchard, Ed.). Seattle: University of Washington Press, pp. 430-442.
- Bradley, E.F.** (1972) The influence of thermal stability on a drag coefficient measured close to the ground. *Agricultural Meteorology*, **9**: 183-190.
- Brutsaert, W.** (1975a) A theory for local evaporation (or heat transfer) from rough and smooth surfaces at ground level. *Water Resources Research*, **11**: 543-550.
- Brutsaert, W.** (1975b) The roughness length for water vapor, sensible heat, and other scalars. *Journal of the Atmospheric Sciences*, **32**: 2028-2031.
- Businger, J.A.** (1973) Turbulent transfer in the atmospheric surface layer. In *Workshop on Micrometeorology* (D.A. Haugen, Ed.). Boston: American Meteorological Society, pp. 67-100.
- Businger, J.A., J.C. Wyngaard, Y. Izumi and E.F. Bradley** (1971) Flux-profile relationships in the atmospheric surface layer. *Journal of the Atmospheric Sciences*, **28**: 181-189.
- Chamberlain, A.C.** (1966) Transport of gases to and from grass and grass-like surfaces. *Proceedings of the Royal Society, London*, **A290**: 236-265.
- Chamberlain, A.C.** (1968) Transport of gases to and from surfaces with bluff and wave-like roughness elements. *Quarterly Journal of the Royal Meteorological Society*, **94**: 318-332.
- Chamberlain, A.C.** (1983) Roughness length of sea, sand, and snow. *Boundary-Layer Meteorology*, **25**: 405-409.
- Charnock, H.** (1955) Wind stress on water: An hypothesis. *Quarterly Journal of the Royal Meteorological Society*, **81**: 639.
- Danckwerts, P.V.** (1951) Significance of liquid-film coefficients in gas absorption. *Industrial Engineering Chemistry*, **43**: 1460-1467.
- Danckwerts, P.V.** (1970) *Gas-Liquid Reactions*. New York: McGraw-Hill.
- Deardorff, J.W.** (1968) Dependence of air-sea transfer coefficients on bulk stability. *Journal of Geophysical Research*, **73**: 2549-2557.
- Dennerly, P. and A. Krzywicki** (1967) *Mathematics for Physicists*. New York: Harper and Row.
- Dipprey, D.F. and R.H. Sabersky** (1963) Heat and momentum transfer in smooth and rough tubes at various Prandtl numbers. *International Journal of Heat and Mass Transfer*, **6**: 329-353.
- Duff, G.F.D. and D. Naylor** (1966) *Differential Equations of Applied Mathematics*. New York: John Wiley and Sons.
- Dyer, A.J.** (1974) A review of flux-profile relationships. *Boundary-Layer Meteorology*, **7**: 363-372.
- Garratt, J.R. and B.B. Hicks** (1973) Momentum, heat and water vapour transfer to and from natural and artificial surfaces. *Quarterly Journal of the Royal Meteorological Society*, **99**: 680-687.

- Goldstein, S. (Ed.) (1965) *Modern Developments in Fluid Dynamics*. New York: Dover.
- Grass, A.J. (1971) Structural features of turbulent flow over smooth and rough boundaries. *Journal of Fluid Mechanics*, **50**: 233-255.
- Hibler, W.D. III (1980) Modeling a variable thickness sea ice cover. *Monthly Weather Review*, **108**: 1943-1973.
- Hicks, B.B. and H.C. Martin (1972) Atmospheric turbulent fluxes over snow. *Boundary-Layer Meteorology*, **2**: 496-502.
- Hill, R.J. (1978) Spectra of fluctuations in refractivity, temperature, humidity, and the temperature-humidity cospectrum in the inertial and dissipation ranges. *Radio Science*, **13**: 953-961.
- Kestin, J. and L.N. Persen (1962) The transfer of heat across a turbulent boundary layer at very high Prandtl numbers. *International Journal of Heat and Mass Transfer*, **5**: 355-371.
- Khundzhua, G.G. and Ye.G. Andreyev (1974) An experimental study of heat exchange between the ocean and the atmosphere in small-scale interaction. *Izvestiya, Atmospheric and Oceanic Physics*, **10**: 685-687.
- Kim, H.T., S.J. Kline and W.C. Reynolds (1971) The production of turbulence near a smooth wall in a turbulent boundary layer. *Journal of Fluid Mechanics*, **50**: 133-160.
- Kind, R.J. (1976) A critical examination of the requirements for model simulation of wind-induced erosion/deposition phenomena such as drifting snow. *Atmospheric Environment*, **10**: 219-227.
- Kondo, J. (1975) Air-sea bulk transfer coefficients in diabatic conditions. *Boundary-Layer Meteorology*, **9**: 91-112.
- Large, W.G. and S. Pond (1982) Sensible and latent heat flux measurements over the ocean. *Journal of Physical Oceanography*, **12**: 464-482.
- Leavitt, E., D. Bell, M. Clarke, R. Anderson and C. Paulson (1977) Computation of air stress and sensible heat fluxes from surface layer profile data, AIDJEX, 1975. *AIDJEX Bulletin*, **36**: 157-174.
- Lettau, H.H. (1979) Wind and temperature profile prediction for diabatic surface layers including strong inversion cases. *Boundary-Layer Meteorology*, **17**: 443-464.
- Liu, W.T. and J.A. Businger (1975) Temperature profile in the molecular sublayer near the interface of a fluid in turbulent motion. *Geophysical Research Letters*, **2**: 403-404.
- Liu, W.T., K.B. Katsaros and J.A. Businger (1979) Bulk parameterization of air-sea exchanges of heat and water vapor including the molecular constraints at the interface. *Journal of the Atmospheric Sciences*, **36**: 1722-1735.
- Mangarella, P.A., A.J. Chambers, R.L. Street and E.Y. Hsu (1973) Laboratory studies of evaporation and energy transfer through a wavy air-water interface. *Journal of Physical Oceanography*, **3**: 93-101.
- Maykut, G.A. (1978) Energy exchange over young sea ice in the Central Arctic. *Journal of Geophysical Research*, **83**: 3646-3658.
- Monin, A.S. and A.M. Yaglom (1971) *Statistical Fluid Mechanics: Mechanics of Turbulence*. Vol. 1. Cambridge, Massachusetts: MIT Press.
- Owen, P.R. and W.R. Thomson (1963) Heat transfer across rough surfaces. *Journal of Fluid Mechanics*, **15**: 321-334.
- Parkinson, C.L. and W.M. Washington (1979) A large-scale numerical model of sea ice. *Journal of Geophysical Research*, **84**: 311-337.
- Paulson, C.A. (1970) The mathematical representation of wind speed and temperature profiles in the unstable atmospheric surface layer. *Journal of Applied Meteorology*, **9**: 857-861.
- Pruppacher, H.R. and J.D. Klett (1978) *Microphysics of Clouds and Precipitation*. Dordrecht: Reidel.

- Schlichting, H.** (1968) *Boundary-Layer Theory* (Translated by J. Kestin). Sixth edition. New York: McGraw-Hill.
- Schmidt, R.A.** (1982) Vertical profiles of wind speed, snow concentration, and humidity in blowing snow. *Boundary-Layer Meteorology*, **23**: 223-246.
- Tennekes, H. and J.L. Lumley** (1972) *A First Course in Turbulence*. Cambridge, Massachusetts: MIT Press.
- Thorpe, M.R., E.G. Banke and S.D. Smith** (1973) Eddy correlation measurements of evaporation and sensible heat flux over Arctic sea ice. *Journal of Geophysical Research*, **78**: 3573-3584.
- Untersteiner, N. and F.I. Badgley** (1965) The roughness parameter of sea ice. *Journal of Geophysical Research*, **70**: 4573-4577.

A facsimile catalog card in Library of Congress MARC format is reproduced below.

Andreas, E.L

A theory for Scalar roughness and the scalar transfer coefficients over snow and sea ice / by Edgar L Andreas. Hanover, N.H.: Cold Regions Research and Engineering Laboratory. Springfield, Va.: available from National Technical Information Service, 1986.

vi, 28 p., illus.; 28 cm (CRREL Report 86-9.)

Prepared for Office of the Chief of Engineers by Corps of Engineers, U.S. Army Cold Regions Research and Engineering Laboratory under DA Project 4A161102-AT24.

Bibliography: p. 17.

1. Heat and moisture exchange. 2. Roughness lengths. 3. Sea ice. 4. Snow. 5. Surface processes. 6. Turbulence. I. United States. Army. Corps of Engineers. II. Cold Regions Research and Engineering Laboratory, Hanover, N.H. III. Series: CRREL Report 86-9.

END

1-87

DTIC